La Metallurgia Italiana
International Journal of the Italian Association for Metallurgy

Research and practice on improving the oxygen content of welding steel wire rod ER70S-6

T. Chen, M. Yi, Y. Liu, X. Zhang, H. Luo

The effect of deoxidation process during tapping on the non-metallic inclusions control in welding steel ER70S-6 is investigated in this paper, especially two different deoxidizing process were applied to obtain high oxygen content, and the characteristic of inclusions were studied and compared. To produce ER70S-6, aluminum containing deoxidizers are generally charged into molten steel during tapping, thereby stable alloy yield and high steel cleanliness could be achieved. However, the product of aluminum deoxidization is Al2O3 with high melting point and high elastic modulus, which leads to drawing crack and nozzle clogging. Nozzle clogging is also harmful to the steel cleanliness, and finally resulting in economic losses and production safe. In this study, the effect of Al-Si-Mn complex deoxidation was investigated. Although the amount of inclusions increased significantly from 66.4 to 213.5 per square millimeter, the inclusion type changed to silicate with lower elastic modulus, and the average diameter decreased from 1.32μm to 1.09μm, which both ensured the good drawing performance of ER70S-6 wire rod. Furthermore, considering that oxygen element could reduce molten steel surface tension and viscosity, the amount of oxygen under the new deoxidation process increases to more than 60ppm and 100ppm which is 3 times than original process, and it is more favorable for the welding performance, such as improving soldering seam formation and reducing metal spattering. The ER70S-6 wire rod produced by the new process has reached a few thousands tons, and there were no defects during subsequent works.

KEYWORDS: OXYGEN CONTENT, INCLUSION, WELDING WIRE ROD, ER70S-6

INTRODUCTION

Oxygen and sulfur exist as non-metallic inclusions in steel, which are the main factors causing fractures during the drawing process of wire rods, especially oxide inclusions with large size and poor deformation ability[1-8]. ER70S-6, a typical welding steel wire rod, is generally controlled to have an oxygen content of no more than 30ppm to have better cleanliness, thus to reduce drawing fracture. On the other hand, oxygen and sulfur are surface active elements that exist in appropriate amounts in welding steel, which can reduce the splashing of large particles in the corresponding welding wire. It is beneficial for welding performance[9]. Additionally, small-sized inclusions are also beneficial for improving the performance of the deposited metal. Therefore, increasing the oxygen content in steel while eliminating the influence of inclusions on the drawing performance

Tao Chen, Min Yi, Yangyang Liu,
Xin Zhang, Hongjin Luo
Shougang Group Co. Ltd, & Beijing Key Laboratory of Green Recyclable Process for Iron and Steel Production Technology, China - 34542363@qq.com

is good to the quality of welding steel wire rod. As to characteristic parameters of the inclusions, the size, the type, the quantity,and the distribution are all need to be paid attention to. Scanning electron microscopy (SEM) is usually used to detect the inclusions in steel[10-13]. Combined with its energy spectrum analysis, the detection and analysis of the above characteristic parameters can be carried out simultaneously.

In the production of ER70S-6 wire rod in Shougang Group, two different oxygen content levels of 60ppm and 100ppm were obtained by adjusting the producing process. Two types of refining process were used to control the inclusions, such as the type, the quantity, and the size. The inclusions under two different processes were analyzed and compared.

EXPERIMENTAL MATERIALS

The samples in this study were taken from industrial production of ER70S-6 wire rods. The main production process is EAF → refining process → continuous casting with full protection (150mm × 150mm cross section billet) → high-speed wire rolling (wire rod with a diameter of 5.5mm) → controlled cooling. Two types of refining processes, ladle refining (hereinafter referred to as LF) and bottom blowing argon (hereinafter referred to as AB), were used desperately, while other processes operations were same. The amount of Al-contained deoxidizer was different either, which used in AB process is less than that of LF process.

Samples were taken randomly from each process. The main compositions were analyzed by ICP(Inductively Coupled Plasma Atomic Emission Spectrometer) and an oxygen nitrogen analyzer. The results are listed in Tab. 1.

Tab.1 - Compositions of ER70S-6 wire rods produced by two process,%.

Process	Sample No.	C	Si	Mn	P	S	Al	T.O	N
AB	1	0.070	0.90	1.48	0.012	0.0095	<0.002	0.0110	0.0065
LF	2	0.072	0.87	1.50	0.013	0.012	0.005	0.0062	0.0069

By comparison, it can be seen that the main difference in the composition of two samples is the content of aluminum and oxygen. Aluminum is lower and oxygen is higher in sample 1 which is produced by AB process, while it's opposite in sample 2 by LF process.

EXPERIMENTAL METHODS

Inclusions of the wire rod samples were observed under a multifunctional desktop scanning electron microscope (Phenom XL G2). The composition, quantity, size, and position distribution of inclusions in each sample were detected and statistically analyzed using the Feature function. The field of view position is shown in Fig. 1.

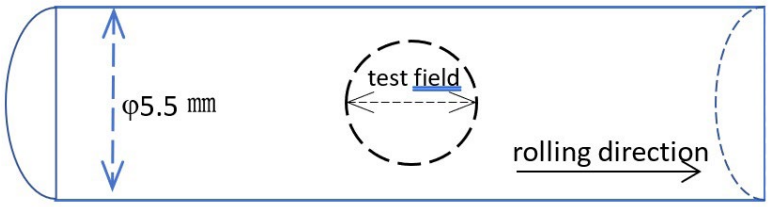

Fig.1 - Schematic diagram of inclusion detection field in the longitudinal section of wire rod sample.

The area of one testing field is about 0.32mm^2. The total area of testing fields of every sample is about 5.5mm^2.

RESULTS & ANALYSIS

Amount and type of inclusions

Tab. 2 lists the quantities of various types of inclusions in the samples.

Tab.2 - Type & amount of inclusions.

Inclusions Type	Sample 1	Sample 2
Ca-Al-Si-Mn-O (Ca-Al-Si-O-MnS)	99	108
Ca-Si-Mn-O (Ca-Si-Mn-O-MnS)	11	6
Al-Si-Mn-O (Al-Si-Mn-O-MnS)	607	28
Al-O (Al-O-MnS) & MgO·Al2O3	0	6
Si-Mn-O (Si-Mn-O-MnS)	440	202
(single) MnS	17	15
Total	1174	365

The types of inclusions in the wire rod are basically the same in both processes, various types of oxides, sulfides and their mixtures, but different in amount. For ER70S-6 steel, the deoxidation process in production practice is actually a composite deoxidation of Al, Si, and Mn. Therefore, the deoxidation products should be oxides and their mixtures of Al, Si, and Mn. Most of the Ca comes from the evolution under the influence of refining slag, and a very small amount comes from the introduction of alloys such as SiFe. Comparing the same type of inclusions under two different processes, it can also be seen that more inclusions in sample 2 are affected by Ca, such as Al-Si-Mn-O particles, which transform into Ca-Al-Si-Mn-O in a higher proportion and quantity, consistent with the process. It could be calculated that the amount of inclusions increased significantly from 66.4 to 213.5 per square millimeter

Fig. 2 shows the statistical results of oxides and sulfides under two different process routes.

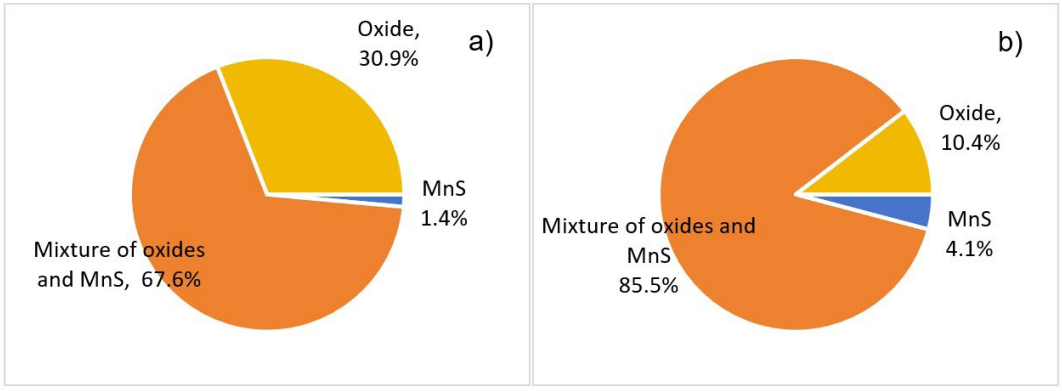

Fig.2 - Statistics of Inclusion Types in ER70S-6 Wire Rods a) Sample 1, b) Sample 2.

It is shown that under the two process routes, the types of inclusions in the wire rod are basically the same, mostly a mixture of various types of oxides and sulfides, followed by various types of oxides, and pure compound MnS only exists in a very small amount. Due to different deoxidation processes, there are small amounts of alumina and magnesium aluminum spinel particles in sample 2. This type of inclusion was not found in sample 1. In addition, the proportion of the mixture in sample 2 is much higher than that in sample 1, which corresponds to the comparison of the number of oxide and sulfide inclusions.

Fig. 3 shows the quantity and proportion of various types of inclusions. Here the mixture is included in the corresponding oxides, and MnS is only included in the pure amount.

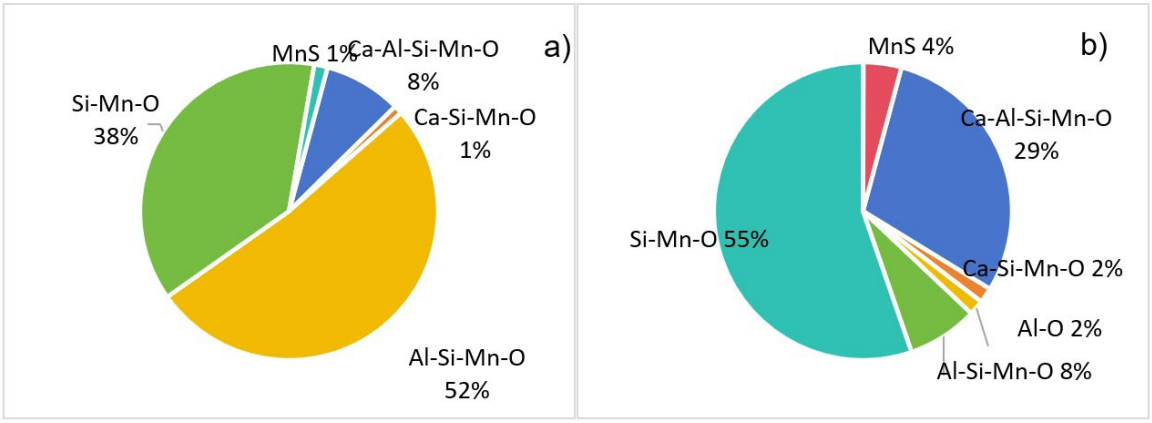

Fig.3 - Quantity of Different Types of Inclusions in ER70S-6 Wire Rod a) Sample 1, b) Sample 2.

It is shown from the statistical results that the various oxide inclusions in Samples 1, in desending order of quantity, are Al-Si-Mn-O, Si-Mn-O, Ca-Al-Si Mn-O, and Ca-Si-Mn-O. The first two types are accounting for approximately 89% in total. Listed in the same way of sample 2, they are Si-Mn-O, Ca-Al-Si-Mn-O, Al-Si-Mn-O, Ca-Si-Mn-O, and Al (Mg) - O. The first two types are accounting for about 85% in total.

COMPOSITIONS OF INCLUSIONS

The content of main elements, such as Ca, Al, Si, and Mn, of various types of inclusions are shown in Fig. 4.

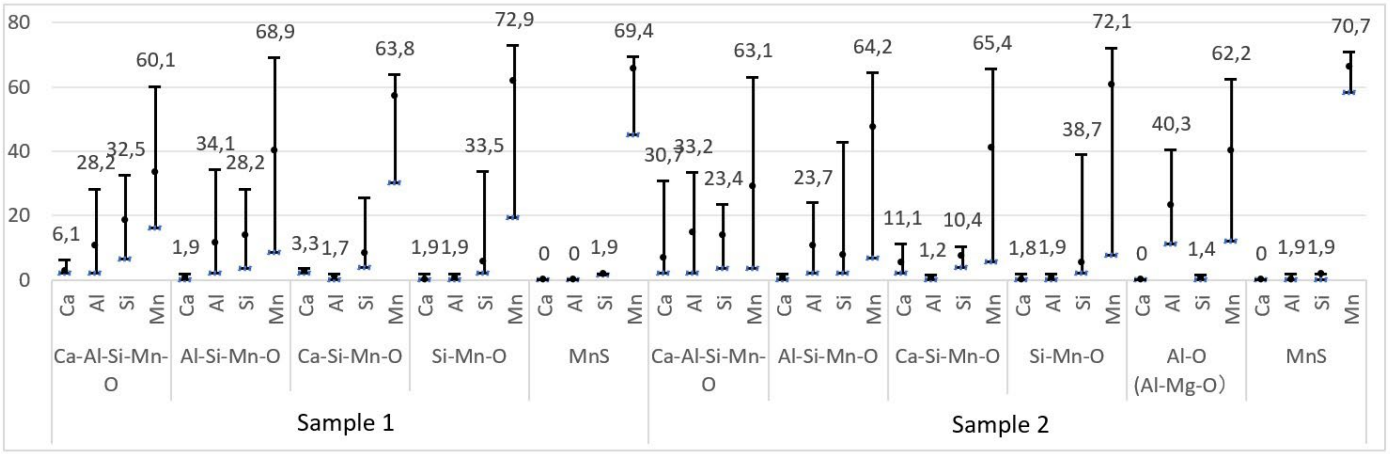

Fig.4 - Main Element Content of Various Types of Inclusions in ER70S-6 Wire Rod.

It can be seen that: Firstly, Al, Si, and Mn are the main elements in the inclusions, and even particles containing Ca have lower Ca content, especially in sample 1, which is further reduced compared to sample 2. Secondly, in terms of Si content in particles of the same type of inclusion, the average of sample 1 is slightly lower than that of sample 2. Thirdly, in Ca-Al-Si-O and Al-Si-O type inclusions, the Al content in sample 2 is high and Si is low, while in sample 1, Si is high and Al is low, which is consistent with the deoxidation process (Al content in the steel).

The elements in the inclusions are mainly Al, Si, and Mn. Even those particles containing Ca, the Ca content is relatively low, especially in sample 1, which is further reduced compared to the sample 2. As to the Si content in the same type of inclusions, the average value of sample 1 is slightly lower than that of sample 2. In Ca-Al-Si-Mn-O and Al-Si-Mn-O inclusions, the Al content in sample 2 is high and Si is low. However in sample 1, Si is high and Al is low. This is consistent with both the deoxygenation process and Al content in the steel.

SIZE OF INCLUSIONS

Tab. 3 lists the size of various types of inclusions in the samples under two different processes.

Tab. 3 - Size of each type of inclusion in ER70S-6 Wire rod

Tab.1 - Caratteristiche disponibili e ricavate dei materiali carboniosi considerati (la definizione della tipologia di materiale corrisponde a quella fornita dal fornitore).

	Sample 1					Sample 2					
	Ca-Al-Si-Mn-O	Ca-Si-Mn-O	Al-Si-Mn-O	Si-Mn-O	MnS	Ca-Al-Si-Mn-O	Ca-Si-Mn-O	Al-(Mg)-O	Al-Si-Mn-O	Si-Mn-O	MnS
Max	7.346	1.312	4.284	3.636	3.084	6.501	6.596	4.835	6.217	2.181	2.809
Min	0.636	0.551	0.581	0.551	0.842	0.711	0.801	0.918	0.687	0.519	0.757
Ave	1.302	0.915	1.22	1.005	1.234	1.583	2.126	2.338	1.457	0.949	1.376

The average size (hereinafter referred to as ECD, equivalent calculated diameter) of inclusions is based on the assumption that all inclusions are spherical. ECD of most types of inclusions in sample 1 is smaller than that in sample 2, only Si-Mn-O inclusions are slightly larger. Si-Mn-O inclusions are the only type with a larger amount shared by the two samples. It is also the smaller size inclusion type among all existing types. Total calculated, the inclusions average size of sample 1 is 1.09μm, and it's much smaller than sample 2, which average size is 1.32μm. Fig.5 shows the distribution of various types of inclusions size.

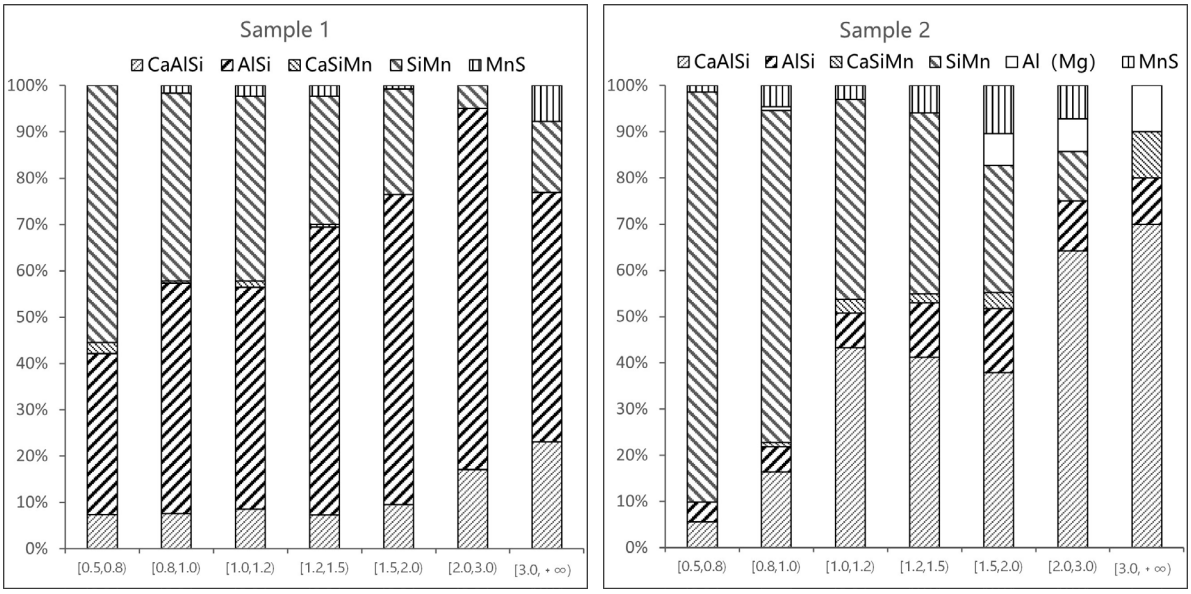

Fig.5 - Size distribution of various types of inclusions.

It can be seen that the size distribution of inclusions under the two processes has both similarities and differences according to their types. Those aspects with similar characters include: if calcium modification is not considered, small-sized inclusions are mainly Si-Mn composite deoxygenation products. As the size increases, inclusions gradually transition to Al-Si-Mn type, but there are differences in the specific proportion.

As to sample 1, small-size (<0.8μm) inclusions are mainly Si-Mn-O type, but the proportion of Al-Si-Mn-O type has significantly increased when the size is greater than 0.8μm. As to sample 2, the small-sized (<1.0μm) inclusions are Si-Mn-O type. When the size is in the range of 1.0μm and 1.5μm, the proportion of Si-Mn-O type and Al-Si-

Mn-O type is basically equivalent. Inclusions with a size of ≥1.5μm is mostly the Al-Si-Mn-O type in quantity, while Al oxides and spinel inclusions also appear;

The differences also include: the effect of calcium treatment is more obvious on sample 2, so it can be seen that sample 1 still mainly belongs to the type before calcium treatment, which is related to the different refining process cycles. It can be found that the modification effect of calcium is more prominent on the type of Al-Si-Mn-O, while the Si-Mn-O type is less affected, only showing performance on larger sized inclusion particles, In fact, the Al-Si-Mn-O type also shows a trend of increasing the proportion of modification with increasing size, which is also the effect of calcium on the modification of inclusions, forming lower melting point inclusions, increasing size, and making them easier to float and remove. In general, Ca treatment has more obvious influence on larger-sized inclusions.

DISLOCATION OF INCLUSIONS

Fig.6 plot the positions of relatively large amounts of Si-Mn-O, Ca-Al-Si-O, and Al-Si-O types (including mixtures) inclusions of both samples.

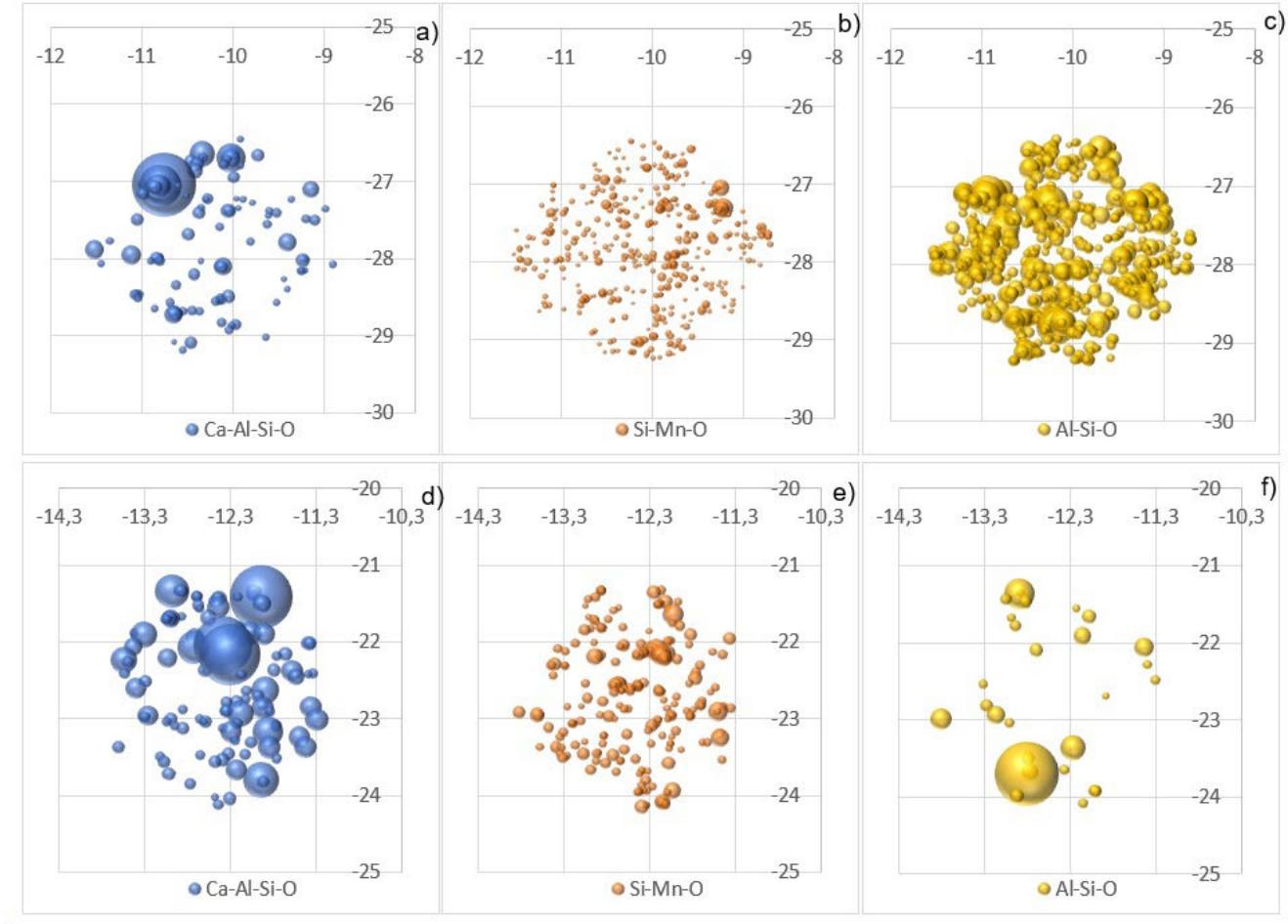

Fig.6 - Distribution of Main Types of Inclusions in ER70S-6 Wire Rod a,b,c) Sample 1; d,e,f) Sample 2.

As shown in the fig.6, the distribution of various types of inclusions in the wire rod can be considered random or even. It can also be more intuitively observed that compared to sample 1, more Al-Si-O inclusions in sample 2 transform into Ca-Al-Si-O.

DEFORMATION OF INCLUSIONS

During rolling, the inclusions extend as steel transforms. The deformation rate, here which is defined as the maximum diameter of inclusion particle divide the minimum diameter (Dmax/Dmin), is closely related to the elastic modulus of inclusions[14,15]. It is found that this

deformation rate is also related to the size of inclusions, as shown in fig.7.

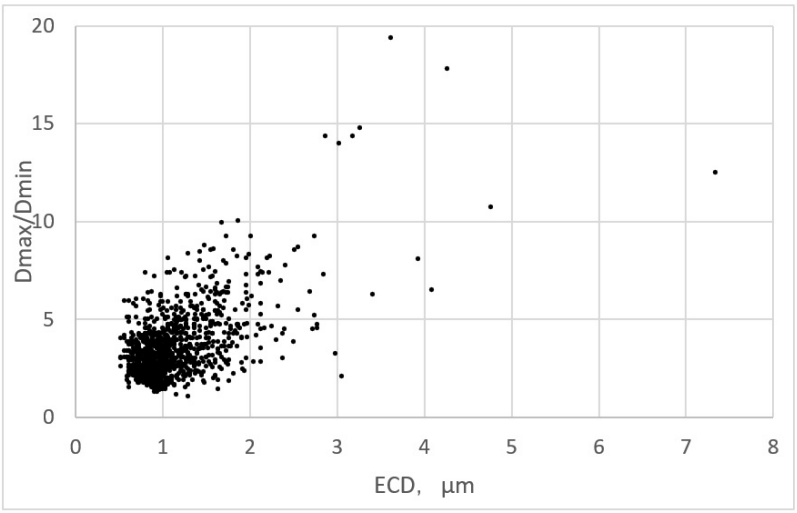

Fig.7 - Relation of the inclusions deformation rate during steel rolling and the inclusion size.

It can be seen that, in general the smaller the inclusion is, the more difficult to deform. The deformation of inclusion particles during hot rolling may be influenced by both their type and original size. It is inferred that larger particles are significantly affected by size, while smaller particles are significantly affected by type.

Vertical to the rolling direction, the test field is divided into five groups, and each group is named sequentially from 1 to 5, as shown in fig. 12. The statistical results of inclusions deformation rate of each sample under two refining process are also illustrated in fig.8.

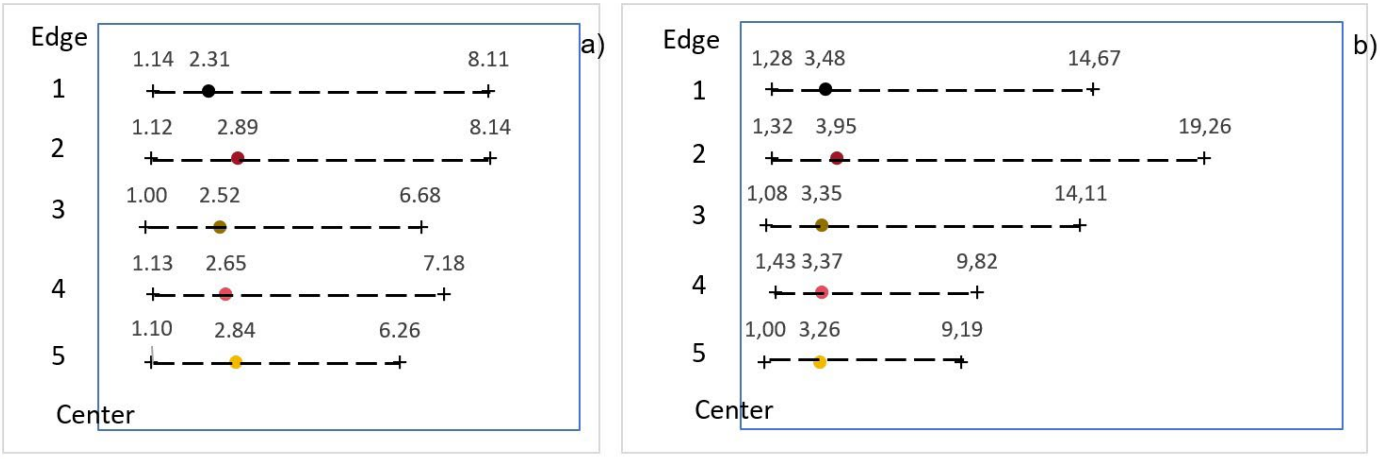

Fig.8 - Deformation of inclusions in the radial grouping field of view a) Sample 1, c) Sample 2.

The inclusion amount per unit area of each group was also counted, however from the statistical results, it can be seen that there is no obvious pattern in the distribution of radial inclusions.

From the statistical results, it can be seen that: 1) on a single sample, under two refining processes, the elongation deformation rate of inclusions in each group after radial grouping does not show a significant correlation with the position of each group; 2) Comparing the two refining processes, the deformation rate of inclusions in the coil

under the Ar blowing process is relatively high, which should be related to the small original size of inclusions in the sample, and also supports the previous analysis of fragmentation during inclusion rolling process.

Based on the above analysis, it is believed that for this type of small-sized wire rod (ϕDue to the large compression ratio (about 948), the elongation deformation at the edges and center of the steel billet is significant, masking the differences in surface deformation. Some studies have also found that during rolling, due to the dragging effect of the rolls on the surface position, the actual maximum deformation position is at R/2, which is inconsistent with the conclusion of this experiment. Therefore, further research is needed in this direction.

CONCLUSIONS

Thousands of tons of ER70S-6 wire rods have been produced in the above experimental process, and the whole production goes smoothly.

The success rate of steelmaking by experimental process is 100%, the pass rate of billetes is more than 99%, and the yield rate of wire rods exceeds 97%. All of the economic and technical indicators are equivalent to conventional process.

In terms of usage, the drawing performance of the wire rod is excellent, and no abnormal drawing fracture has been reported.

The oxygen content in ER70S-6 wire rods produced in experimental process is about 110ppm, which is almost two or three times of that of conventional process.

Oxygen in welding electrods is beneficial for welding performance as it can reduce welding spatter, increase the aspect ratio of the weld seam, and form a wide weld seam. More research will be carried out on welding performance of experimental ER70S-6 based on this research work.

BIBLIOGRAFIA

[1] Chen ZL, Wang X, Fan BH, Li N. Summary and Analysis of the Causes of SWRH82B Wire Rod Drawing Fracture. Shanxi Metallurgy. 44(05), 2021. p. 205-207.
[2] Xiao MD, Li FQ, Luo XZ, Zhu XR, Zhang YC, Zhang ZY. Cause analysis of the fracture occurrence during the drawing of SWRCH22A cold heading wire rod. Jiangxi Metallurgy. 5, 2020. p. 40-44.
[3] Han XQ, Du DC, Xie FF, Sun XY. Cause analysis of the fracture occurrence during the drawing of YL82B wire rod. MW Metal Forming. 12, 2018. p. 66-68.
[4] Ling HC, Li JC, Bai WP, Yang BJ. Analysis about drawing break of welding-wire H11Mn2SiA steel wire bar. Hebei Metallurgy. 8, 2016. p. 70-73.
[5] Nong ZJ, Liu CL, Liu JY, Wu DX. Analysis on drawing fracture of SWRM17 caused by inclusions. Southern Metals. 5, 2015. p. 44-46.
[6] 6. Wang KP, Wang Y, XU JF, Chen TJ, Xie W, Jiang M. Investigation on evolution of inclusions in bearing steel during secondary refining. Iron and Steel. 6, 2022. p. 1-8.
[7] Wang QB, Zhang H, Li YC, Lu CL, Bai RJ, Liu CS. Effect of 120t LF refining slag system on plasticity inclusions in 55SiCrA Spring Steel. Special Steel. 43(01), 2022. p. 34-38.
[8] Zhu MY, Deing ZY. Evolution and control of non-metallic inclusions in steel during secondary refining process. Acta Metallurgica Sinica. 58(01), 2022. p. 28-44.
[9] Li Xiaona(translated). New welding wire for thin steel sheet. Modern Welding Technology. 10, 2010. p. 32-35.
[10] Li L, Wu XD, Yang LW. Research on inclusions of 48MnV microalloy steel. China Steel Focus. 3, 2022. p 25-27.
[11] Wu H, Deng XT, Li CR, Sui Y, Zhang T, Ji WB, Wang ZD. Analysis on cold bending fracture of wear-resistant steel NM400. Heat Treatment of Metals. 46(09), 2021. p. 262-267.
[12] Wang DX, Li ZW, Xie JB, Wang Y, Fu JX. Analysis on cause of 23MnNiCrMo54 steel chain breaking. Shanghai Metals. 43(01), 2021. p. 113-118.
[13] Long H, Cheng GG, Qiu WS, Zeng LY, Yu TH, Liu D. Characteristics, sources analysis of large size inclusions and technical improvement during bearing steel production. China Metallurgy. 30(09), 2020. p. 53-59.
[14] Zhang LF, Guo CB, Yang W, Ren Y, Ling HT. Deformability of oxide inclusions in tire cord steels. Metallurgical and Materials Transactions B. 49B(2), 2018. p. 803-811.
[15] Wang KP, Jiang M, Wang XH, Wan WH, Wang Y. Behavior of Dual-Phase (MnO-SiO2-Al2O3) + (SiO2) Inclusions in Saw Wire Steels during hot rolling and cold drawing. Metallurgical and Materials Transactions B. 51B, 2020. p.95-101.

TORNA ALL'INDICE >